Hindawi Publishing Corporation
International Journal of Distributed Sensor Networks
Volume 2013, Article ID 280186, 7 pages
http://dx.doi.org/10.1155/2013/280186

Research Article

Field Measurement of Wind Effects of Roof Accessory Structures on Gable-Roofed Low-Rise Building

Peng Huang, Ming Gu, Chun-guang Jia, and Da-long Quan

State Key Laboratory of Disaster Reduction in Civil Engineering, Tongji University, Shanghai 200092, China

Correspondence should be addressed to Ming Gu; minggu@tongji.edu.cn

Received 4 July 2013; Accepted 13 August 2013

Academic Editor: Ting-Hua Yi

Copyright © 2013 Peng Huang et al. This is an open access article distributed under the Creative Commons Attribution License, which permits unrestricted use, distribution, and reproduction in any medium, provided the original work is properly cited.

The components and claddings of low-rise buildings are usually destroyed first during typhoon disasters in coastal areas. Roof accessory structures can change the flow pattern on the roof, thus effectively reducing the wind load on the roof surface and the damage to the low-rise buildings. Three types of aerodynamic mitigation plates, that is, (1) 0.3 m high full-length roof-edge plate, (2) 0.3 m high and 0.5 m + 0.5 m long roof-corner plate, and (3) discrete roof-edge plates with different spaces (which can be used as advertisement boards), are studied on the basis of the field measurement results under roof pitches of 10° and 18.4°. By comparing the results of the roof with and without constructed plates, it is implied that the three types of plates can affect the formation of conical vortexes and can significantly reduce the mean and fluctuating pressure coefficients in the windward corner. Compared with the constructed plate, the roof ridge has a larger influence on the wind loads on leeward roof.

1. Introduction

Recent natural calamity investigations show that wind-induced disasters cause large economic losses and many casualties worldwide annually. Most of these losses are related to damages in residential, industrial, and other low-rise buildings. Many notable full-scale studies of wind loads on low-rise buildings have been conducted, which helps to compare their results with wind-tunnel test and numerical simulations. In 1974, the Building Research Establishment in the United Kingdom initiated a program of full-scale measurements on a special constructed experimental building in Aylesbury, England [1]. The building has two stories, 13.3 m in length and 7 m in span. The roof of the building can be adjusted between 5° and 45°. In the late 1980s, the TTU experiment, a famous full-scale experiment on a low-rise building, was conducted in Lubbock, TX, USA [2]. The building was 13.7 m in length, 9.1 m in span, and 4 m in height. Almost at the same time, the United Kingdom established a full-scale model in Silsoe comprising a steel frame building, which is 24 m in length, 12.9 m in span, and 3 m in height. The above experiment is called the Silsoe experiment [3]. Then, a 6 m cube was constructed at the Silsoe Research Institute at the beginning of the 21st century [4]. In China, Hunan University developed a set of field measurements for wind effect on a low-rise building [5]. This low-rise building can be moved to the landing position of typhoons to enable field measurement during typhoons.

Many factors can affect the distribution of wind pressure on buildings, such as geometric shape, size of the building, roof covering, and openings on the wall [6]. Stathopoulos [7] found that the maximum negative pressures (suction) occur at the edges and corners of the roof because of the flow separation. Stathopoulos and Baskaran [8] learned that isolated parapet has little effect on reducing the mean pressure coefficient and the pressure peak in the roof corner. In another study, Kopp et al. [9] elaborately examined the wind effects on the flat roof parapets of low-rise buildings and the wind loads on the parapets. They found that the magnitude of wind loads and their distribution largely depend on the architectural detail. Recently, Blessing et al. [10] assessed the effectiveness of aerodynamic edge devices in reducing wind effects over the roof corners and edge regions of the Wall of Wind (WoW), a large-scale six-fan testing facility. Suaris and Irwin [11] investigated the effectiveness of parapets mounted at the roof edge on mitigating peak suction near the roof corners of the low-rise buildings. Bitsuamlak et al. [12]

Figure 1: Full-scale low-rise test building.

studied some simple architectural elements for reducing high-wind-induced suction occurring at the roofs and wall corners of low-rise buildings in a boundary-layer wind tunnel and in the WoW.

A field laboratory has been set up near Shanghai Pudong International Airport by the State Key Laboratory of Disaster Reduction in Civil Engineering of Tongji University to study the turbulence characteristics of near-ground wind and wind loads on full-scale low-rise buildings. The plane size of the building is 10 m × 6 m, and the eave height is 8 m. The main feature of this building is that the roof pitch can be adjusted from 0° to 30° by using a lifting device. The architectural appearance of the pitch-adjustable building was designed according to the typical characteristics of the low-rise buildings in villages of South China. The pitch-adjustable building has roof accessory structures (aerodynamic wind-resistance devices) installed in the roof to measure the wind loads on the roof and the wind-resistance effect. Some of the results are valuable for the wind-resistance design of low-rise buildings in the coastal regions.

2. Experimental Apparatus Equipment and Data Processing Method

Pudong New District in Shanghai is an area where strong winds, particularly strong typhoons, frequently occur each year. The field laboratory is located in a flat area close to the estuary of the Yangtze River and near the Shanghai Pudong International Airport. The field laboratory consists of a test building and two meteorological towers. The steel-structure test building is 10 m in length, 6 m in width, and 8 m in eave height. The test building features an adjustable roof pitch ranging from 0° to 30°. Figure 1 shows an image of the full-scale building.

A mechanical anemometer (R. M. Young 05305) and an ultrasonic anemometer (R. M. Young 81000) were installed in a 10 m high meteorological tower, which is located about 25 m to the east of the pitch-adjustable building. The ultrasonic anemometer can be used to measure the wind velocity of the standard point. These two anemometers were employed for mutual correction to provide real and effective wind velocity data [13].

There are two types of pressure transducers that were used to measure the surface pressures on the roof of the test building. These transducers are all developed by Kunshan Shuangqiao Sensor Measurement Controlling Co., Ltd. A total of 94 microdifferential pressure sensors with the range of ±1 kPa (CYG1220) were mounted to measure the wind pressure without rain. A total of 20 diaphragm pressure sensors with the range of ±2.5 kPa (CYG1516) were installed under the roof to study the wind-rain-induced effects on pressure [14]. The photos of the two types of transducers are shown in Figure 2.

The southeastern wind is the prevailing wind direction in Shanghai, based on the wind rose of this city. Therefore, more transducers are placed at the southeastern corner [15]. The locations of the pressure taps are shown in Figure 3. The detailed information of the field measurement laboratory, the installed equipment, and the low-rise building model can be found in the paper of Huang et al. [16].

The sample frequency of the anemometer and wind-pressure data acquisition is 20 Hz, and the sampling duration adopted for each data record is 10 min. The wind-pressure coefficient on the roof surface is defined as

$$C_{p_i} = \frac{p_i - p_\infty}{0.5\rho v^2}, \tag{1}$$

where p_i is the pressure of tap i, p_∞ is a static reference pressure and is obtained by the static system that extends to a box below the outdoor ground through a long tube, and v denotes the reference wind velocity measured by the anemometer at the top of the 10 m high meteorological tower near the building. The mean and fluctuating pressure coefficients are then defined by the average value and standard deviation of the pressure coefficient time series; that is,

$$C_{p_i,\text{mean}} = \text{mean}\left(\frac{p_i - p_\infty}{0.5\rho v^2}\right),$$
$$C_{p_i,\text{rms}} = \text{std}\left(\frac{p_i - p_\infty}{0.5\rho v^2}\right). \tag{2}$$

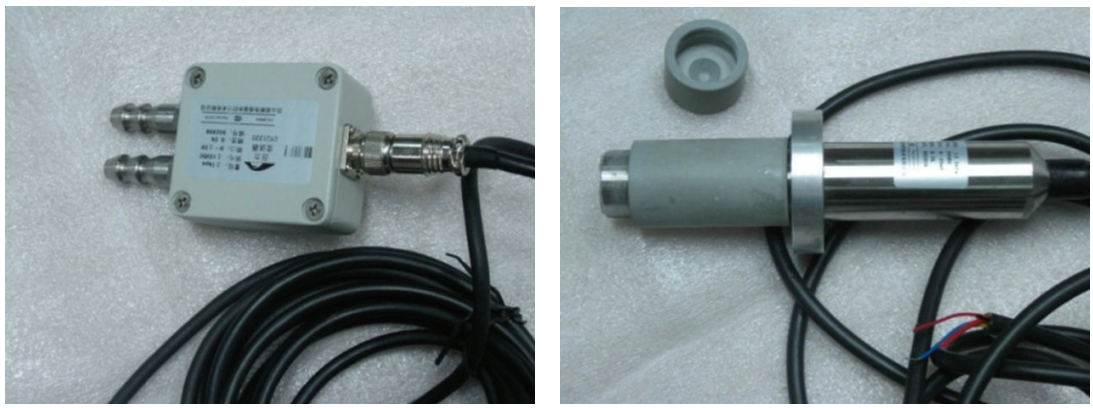

(a) CYG1220 (b) CYG1516

Figure 2: Photos of two types of pressure sensors.

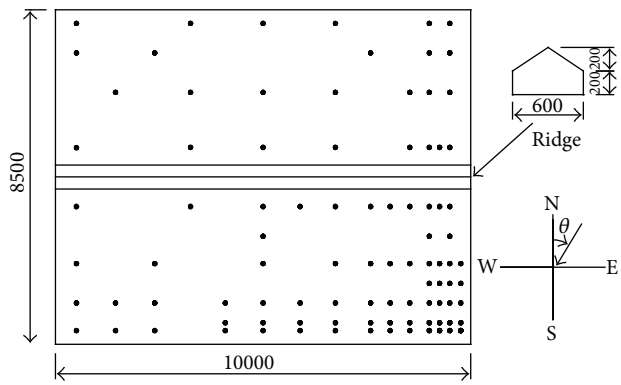

Figure 3: Layout of measuring points on the roof.

3. Test Results and Discussion

3.1. Introduction of Aerodynamic Mitigation Plates and Working Conditions. Because of the short time of field measurement and natural wind direction, only three types of aerodynamic mitigation plates, that is, (1) 0.3 m high full-length roof-edge plate, (2) 0.3 m high and 0.5 m + 0.5 m long roof-corner plate, and (3) discrete roof-edge plates with different spaces (which can be used as advertisement boards), are studied based on the field measurement results under roof pitches of 10° and 18.4°.

In the test, the 0.3 m high full-length roof-edge plate is erected at the northern edge of the roof under a roof pitch of 18.4° (see Figure 4).

The second type of the aerodynamic mitigation plates is used to increase the height of the roof corner, which is 0.3 m high and 0.5 m long in both sides along the roof-edge corner. Considering the wind direction in the field measurement building, the roof-corner plates are erected only in the southeastern corner of the building under a roof pitch of 10° (see Figure 5).

The discrete roof-edge plates include two, three, and four pieces with clear spaces of 2.6, 1.5, and 1.0 m, respectively. These plates are 0.7 m in height and 0.5 m in width and can be used as advertisement boards, which are erected at the southern edge of the roof under a roof pitch of 10° (see Figure 6).

After a period of field measurement, the mean and fluctuating wind-pressure coefficients of each measuring point under natural wind condition are obtained. The effect of these three types of constructed measurement will be discussed below on the basis of the variation of the mean wind-pressure coefficient and fluctuating wind-pressure coefficient before and after the erection of the constructed plate.

3.2. Results of Full-Length Roof-Edge Plate under a Roof Pitch of 18.4°

(a) Mean Wind-Pressure Coefficient. The field measurement results of the building under a roof pitch of 18.4° are obtained. The mean wind-pressure coefficient of the roof without the constructed plate in the 40° wind direction and the roof with the constructed plate in the 35° wind direction are shown in Figure 7.

Figure 7(a) shows the distribution of the mean wind-pressure coefficients on the roof without a constructed plate in the 40° wind direction at a mean wind speed of 10.0 m/s. Because of the effect of the conical vortex in the 40° wind direction, two large negative pressure centers occur on the corner of the windward roof, whose minimum mean wind-pressure coefficients are −2.6 and −1.6, respectively. For the positive wind pressure, the maximum positive pressure coefficient on the windward side is only 0.2. Two negative pressure centers behind the roof ridge emerged on the leeward side; the minimum negative pressure coefficients of these centers are −1.8 and −1.2.

Figure 7(b) shows the distribution of the mean wind-pressure coefficients on the roof with a constructed plate in the 35° wind direction at a mean wind speed of 8.0 m/s. The conical vortex is completely destroyed under the effect of the full-length roof-edge plate, which is located in the windward corner. In addition, the two negative pressure centers in the corner are no longer existing, whereas the

(a) (b)

Figure 4: 0.3 m high full-length roof-edge plate.

(a) (b)

Figure 5: 0.3 m high and 0.5 m + 0.5 m long roof-corner plate.

(a) Two pieces (b) Three pieces (c) Four pieces

Figure 6: Discrete roof-edge plates.

maximum positive pressure coefficient on the windward roof is about 0.6. The leeward roof is mainly influenced by the roof ridge. Therefore, the negative pressure centers behind the roof ridge still exist. The maximum absolute values of the negative pressure centers have increased to some extent because of the air-flow lifting effect of the constructed plate. The differences could also be caused by the 5° difference between the wind direction angle of the field measurement of the roof with a constructed plate and that without a constructed plate.

(b) Fluctuating Wind-Pressure Coefficient. Figures 8(a) and 8(b) show the distribution of the fluctuating wind-pressure coefficients on the roof without and with a constructed plate in the 40° and 35° wind directions, respectively. Similar

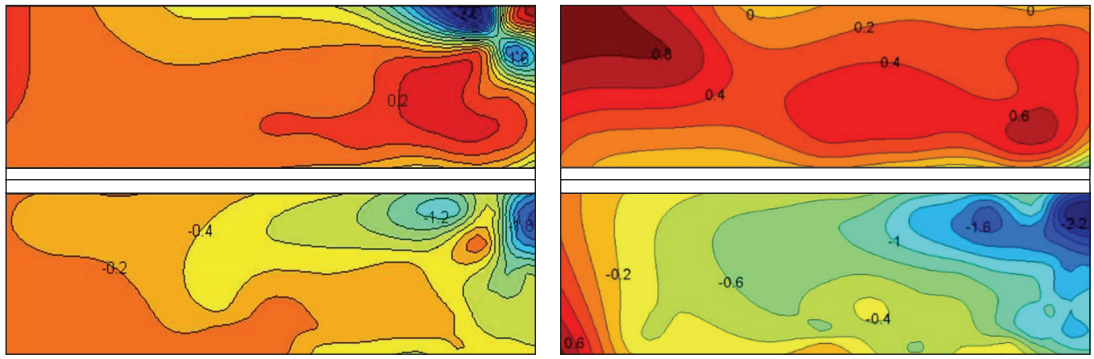

(a) Without a plate in the 40° direction (b) With a roof-edge plate in the 35° direction

Figure 7: Mean pressure coefficients under a roof pitch of 18.4°.

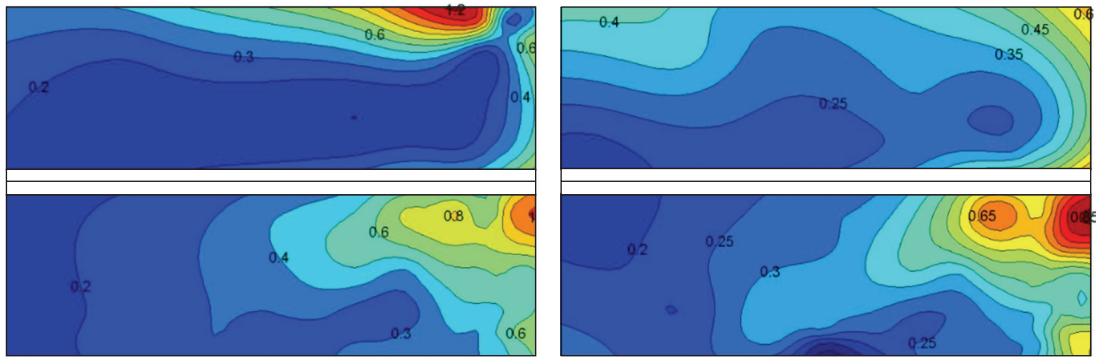

(a) Without a plate in the 40° direction (b) With a full-length roof-edge plate in the 35° direction

Figure 8: Fluctuating pressure coefficients under a roof pitch of 18.4°.

to the distribution of the mean pressure coefficients, two large fluctuating pressure centers occur on the corner of the windward roof without a constructed plate (Figure 8(a)); the maximum pressure coefficients are 1.2 and 0.6. The two pressure centers in the corner no longer exist on the roof with a constructed plate (see Figure 8(b)). The constructed plate can also significantly reduce the fluctuating pressure coefficients in the windward corner.

The maximum fluctuating pressure centers of the leeward roof with a constructed plate decreased to some extent compared with those without a constructed plate.

3.3. Results of the 0.3 m High and 0.5 m + 0.5 m Long Roof-Corner Plate under a Roof Pitch of 10°. The mean pressure results obtained by field measurement for this type of structure are not satisfactory; therefore, only the fluctuating wind pressures on the roof are discussed in this section. As the effect of the roof accessory structures on wind pressure under a small roof pitch is more evident than that of those under a large roof pitch, only the fluctuating pressures on the roof under a roof pitch of 10° are discussed here.

Figure 9(a) shows the field measurement result of the fluctuating pressure coefficient distribution on the roof without a roof-corner plate in the 145° wind direction at a mean wind speed of 10.0 m/s. By comparing the results under a roof pitch of 18.4°, we can observe that the conical vortex becomes more evident in the corner of the windward roof because of the lessened roof pitch. The fluctuating wind-pressure coefficient becomes larger, and two pressure centers occur on the corner of the windward roof, whose maximum fluctuating pressure coefficients are 1.6 and 0.9.

After the erection of the roof-corner plate, when the air flow blows on the structure directly in the 145° wind direction at a mean wind speed of 7.5 m/s, the fluctuating pressure coefficients on both sides of the windward corner become smaller because the corner plate destroys the conical vortex located in the corner (see Figure 9(b)). The maximum fluctuating pressure coefficient is only 1.20, and the position of that coefficient is changed correspondingly.

For the leeward roof, the maximum fluctuating pressure coefficient decreases from 0.6 to 0.4, and the whole fluctuating pressures also decrease at a certain degree before and after the erection of the roof-corner plate.

3.4. Results of the Discrete Roof-Edge Plates under a Roof Pitch of 10°. By considering the effects of roof pitch and the space limitation, we decided to present only the fluctuating pressures of the four pieces of the roof-edge plates with a clear space of 1.0 m under a roof pitch of 10°.

Figure 10 shows the distribution of the fluctuating wind-pressure coefficient on the roof without and with roof-edge plates in 180°, 170°, and 160° wind directions. Figures 10(a),

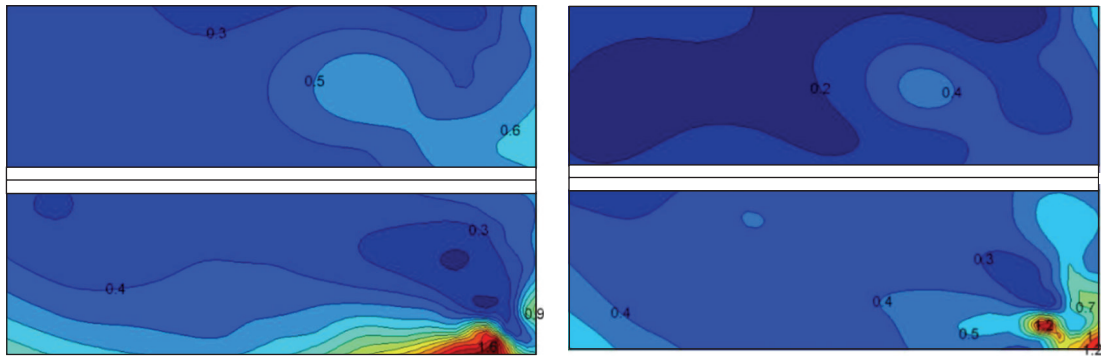

(a) Without a plate in the 145° direction (b) With a roof-corner plate in the 145° direction

Figure 9: Fluctuating pressure coefficients under a roof pitch of 10°.

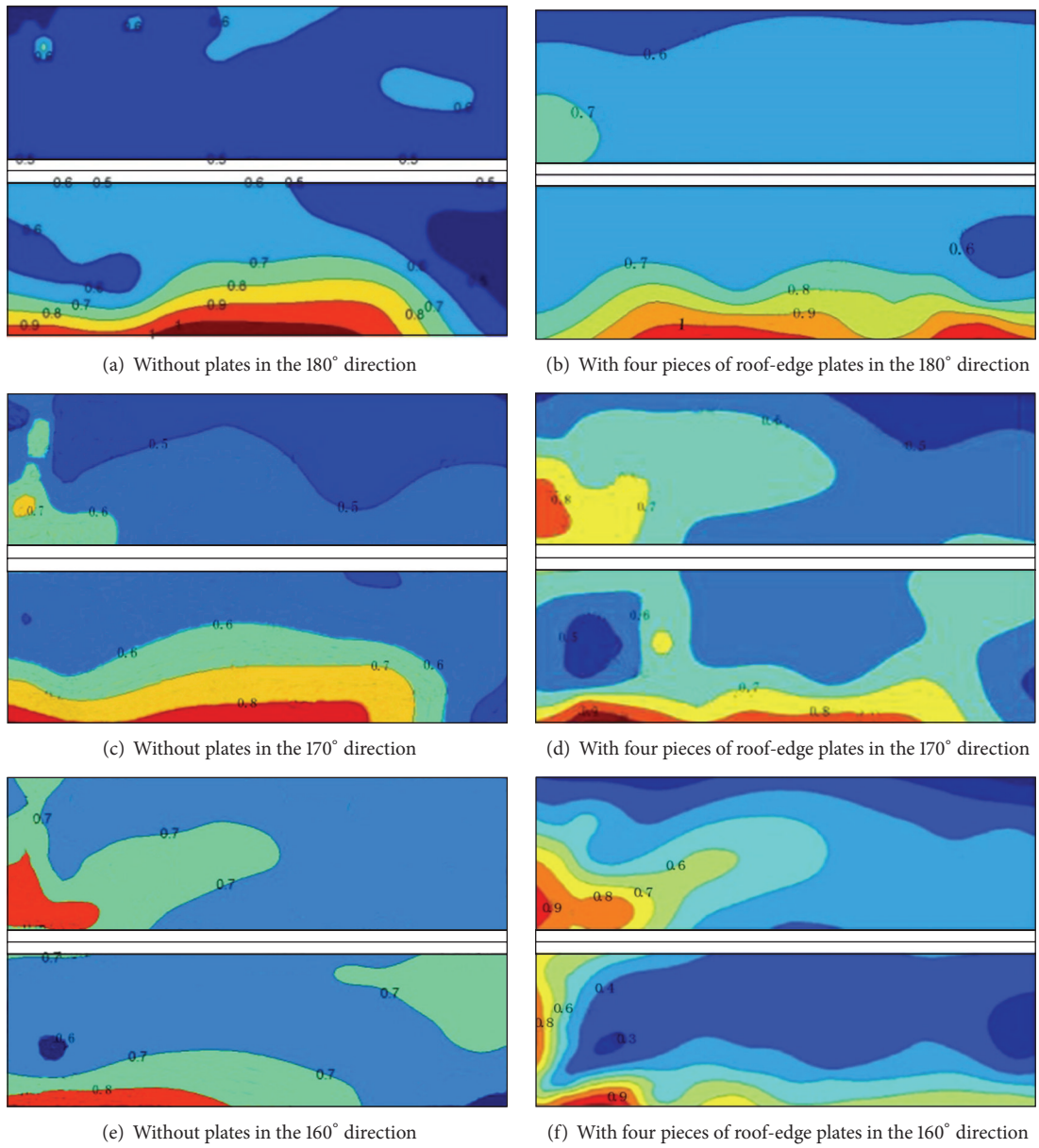

(a) Without plates in the 180° direction (b) With four pieces of roof-edge plates in the 180° direction

(c) Without plates in the 170° direction (d) With four pieces of roof-edge plates in the 170° direction

(e) Without plates in the 160° direction (f) With four pieces of roof-edge plates in the 160° direction

Figure 10: Fluctuating pressure coefficients under a roof pitch of 10°.

10(c), and 10(e) show the cases of the original roof wherein the wind directions are almost normal. The variations of the fluctuating pressure coefficients are mild, and the maximum value is about 1.1. After the erection of the four pieces of roof-edge plates at a mean wind speed of 8.0 m/s, the fluctuating pressure coefficients on the windward roof decrease to some extent (see Figures 10(b), 10(d), and 10(f)). The maximum fluctuating pressure coefficient is about 1.0, and the position of that coefficient is changed correspondingly.

The local fluctuating wind pressures behind the roof-edge plates have increased because of the wake flows by the roof-edge plates.

4. Conclusions

The wind effect of three types of roof accessory structures (aerodynamic mitigation plates) are studied in the paper on the basis of the field measurement of a full-scale low-rise building under roof pitches of 10° and 18.4°. The following conclusions are obtained.

(1) The full-length roof-edge plate has an obvious effect on air-flow lifting, which affects the formation of the conical vortex. Air-flow lifting also results in the effective reduction of the mean and fluctuating wind-pressure coefficients in the windward roof. Compared with the constructed plate, the roof ridge has a larger influence on the wind loads on the leeward roof.

(2) The roof-corner plate can also affect the formation of the conical vortex, which makes the maximum fluctuating pressure coefficient in the corner decrease significantly and the position of that coefficient change correspondingly.

(3) The discrete roof-edge plates can reduce the fluctuating pressure coefficients on the windward roof to some extent. The local fluctuating wind pressures behind the roof-edge plates are increased because of the wake flows caused by the windshield plates.

Conflict of Interests

The authors (Peng Huang, Ming Gu, Chun-guang Jia, and Da-long Quan) declare that there is no conflict of interests regarding the publication of this paper.

Acknowledgment

This paper is supported by the Chinese National Natural Science Foundation (Grants nos. 51178352, 90715040, and 91215302), which is gratefully appreciated.

References

[1] K. J. Eaton and J. R. Mayne, "The measurement of wind pressures on two-storey houses at Aylesbury," *Journal of Industrial Aerodynamics*, vol. 1, pp. 67–109, 1975.

[2] M. L. Levitan and K. C. Mehta, "Texas Tech field experiments for wind loads part 1: building and pressure measuring system," *Journal of Wind Engineering and Industrial Aerodynamics*, vol. 43, no. 1–3, pp. 1565–1576, 1992.

[3] R. P. Hoxey and P. J. Richards, "Full-scale wind load measurements point the way forward," *Journal of Wind Engineering and Industrial Aerodynamics*, vol. 57, no. 2-3, pp. 215–224, 1995.

[4] M. Sterling, C. J. Baker, and R. P. Hoxey, "Short term unsteady wind loading on a low-rise building," *Wind and Structures*, vol. 6, no. 5, pp. 403–418, 2003.

[5] Y. M. Dai, X. G. Yan, X. J. Wang et al., "Statistics and Analysis of typhoons landing and failure mechanism of coastal low-rise buildings in China," *Applied Mechanics and Materials*, vol. 226–228, pp. 1072–1075, 2012.

[6] J. D. Holms, *Wind Loading of Structures*, Spon Press, 2001.

[7] T. Stathopoulos, "Wind pressures on flat roof edges and corners," in *Proceedings of the 7th International Conference on Wind Engineering*, Aachen, Germany, July 1987.

[8] T. Stathopoulos and A. Baskaran, "Turbulent wind loading of roofs with parapet configurations," *Canadian Journal of Civil Engineering*, vol. 15, no. 4, pp. 570–578, 1988.

[9] G. A. Kopp, C. Mans, and D. Surry, "Wind effects of parapets on low buildings: part 4. Mitigation of corner loads with alternative geometries," *Journal of Wind Engineering and Industrial Aerodynamics*, vol. 93, no. 11, pp. 873–888, 2005.

[10] C. Blessing, A. G. Chowdhury, J. Lin, and P. Huang, "Full-scale validation of vortex suppression techniques for mitigation of roof uplift," *Engineering Structures*, vol. 31, no. 12, pp. 2936–2946, 2009.

[11] W. Suaris and P. Irwin, "Effect of roof-edge parapets on mitigating extreme roof suctions," *Journal of Wind Engineering and Industrial Aerodynamics*, vol. 98, no. 10-11, pp. 483–491, 2010.

[12] G. T. Bitsuamlak, W. Warsido, E. Ledesma, and A. G. Chowdhury, "Aerodynamic mitigation of roof and wall corner suctions using simple architectural elements," *Journal of Engineering Mechanics-ASCE*, vol. 139, no. 3, pp. 396–408, 2013.

[13] H. F. Bai, T. H. Yi, H. N. Li, and L. Ren, "Multisensors on-site monitoring and characteristic analysis of UHV transmission tower," *International Journal of Distributed Sensor Networks*, vol. 2012, Article ID 545148, 10 pages, 2012.

[14] T. H. Yi, H. N. Li, and X. Y. Zhao, "Noise smoothing for structural vibration test signals using an improved wavelet thresholding technique," *Sensors*, vol. 12, no. 8, pp. 11205–11220, 2012.

[15] T. H. Yi and H. N. Li, "Methodology developments in sensor placement for health monitoring of civil infrastructures," *International Journal of Distributed Sensor Networks*, vol. 2012, Article ID 612726, 11 pages, 2012.

[16] P. Huang, X. Wang, and M. Gu, "Field experiments for wind loads on a low-rise building with adjustable pitch," *International Journal of Distributed Sensor Network*, vol. 2012, Article ID 451879, 10 pages, 2012.

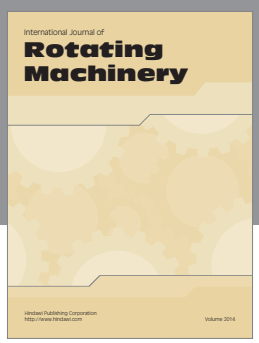

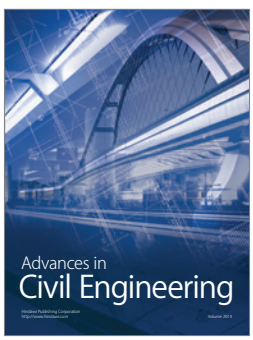

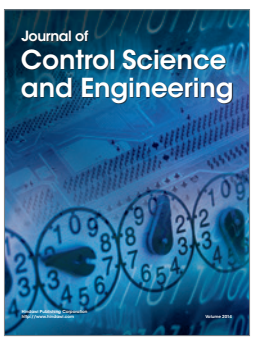

Hindawi
Submit your manuscripts at
http://www.hindawi.com